Superconductivity and Magnetism in Skutterudites

Ctirad Uher

CRC Press
Taylor & Francis Group

Superconductivity and Magnetism in Skutterudites

Superconductivity and Magnetism in Skutterudites

Ctirad Uher

CRC Press
Taylor & Francis Group
Boca Raton London New York

CRC Press is an imprint of the
Taylor & Francis Group, an **informa** business

First edition published 2022
by CRC Press
6000 Broken Sound Parkway NW, Suite 300, Boca Raton, FL 33487-2742

and by CRC Press
2 Park Square, Milton Park, Abingdon, Oxon, OX14 4RN

CRC Press is an imprint of Taylor & Francis Group, LLC

Library of Congress Cataloging-in-Publication Data
Names: Uher, Ctirad, author.
Title: Superconductivity and magnetism in skutterudites / Ctirad Uher.
Description: First edition. | Boca Raton : CRC Press, 2022. | Includes bibliographical references and index.
Identifiers: LCCN 2021044472 | ISBN 9781032116884 (hardback) | ISBN 9781032127200 (paperback) | ISBN 9781003225898 (ebook)
Subjects: LCSH: Skutterudite. | Materials--Thermal properties. | Thermoelectric materials.
Classification: LCC TK2950 .U343 2022 | DDC 621.31/243--dc23/eng/20211108
LC record available at https://lccn.loc.gov/2021044472

ISBN: 978-1-032-11688-4 (hbk)
ISBN: 978-1-032-12720-0 (pbk)
ISBN: 978-1-003-22589-8 (ebk)

DOI: 10.1201/9781003225898

Typeset in Times
by SPi Technologies India Pvt Ltd (Straive)

To my sons Peter and Andrew

Content

Preface

Skutterudites have been the subject of keen scientific studies for the past 40 years or so. The interest was precipitated by the discovery of Prof. Wolfgang Jeitschko and his colleagues (1977), revealing that an open structure of skutterudites typified by two large voids in the unit cell can be filled with foreign species (ions), giving rise to what are called filled skutterudites. Throughout the years, it has been shown that the filling dramatically modifies the physical properties of the original binary form of skutterudites and gives rise to a plethora of fascinating electronic, magnetic, and superconducting characteristics.

The presence of a weakly bonded filler in the oversized void of the crystalline lattice of skutterudites very strongly degrades the ability of the structure to propagate acoustic phonons and, coupled with the outstanding electronic properties (electrical conductivity and the Seebeck coefficient), it resulted in exceptional thermoelectric performance of filled skutterudites that rivals the properties of the best thermoelectric materials. This is particularly so in the temperature range of 500 K–800 K, the regime where industrial processes generate plentiful waste heat that can be harvested and converted to useful electrical energy. The topic of thermoelectric energy conversion using skutterudites has been extensively covered in my book Thermoelectric Skutterudites (2021).

In the present monograph, the emphasis is on exciting developments in superconducting and magnetic properties of skutterudites that followed the initial unexpected detection of a superconducting state in $LaFe_4P_{12}$ with a transition temperature of 4.1 K by Meisner (1981). Since then, the progress has been rapid, and superconductivity has been observed in many other filled skutterudites, including arsenide- and antimonide-based structures, and later in various forms of skutterudites having the $[Pt_4Ge_{12}]$ framework. The superconducting state has often been characterized by a rather high transition temperature that in the case of $La_xRh_4P_{12}$ reached 17 K, Shirotani et al. (2005). Moreover, two skutterudite compounds, $LaFe_4P_{12}$ and YFe_4P_{12}, displayed a highly unusual increase in the transition temperature with applied pressure, DeLong and Meisner (1985) and Cheng et al. (2013), respectively. The climax of the studies was the discovery of a highly exotic and unconventional nature of the superconducting state in $PrOs_4Sb_{12}$, Maple et al. (2002) and Bauer et al. (2002), and subsequently in the Pr-filled $[Pt_4Ge_{12}]$ structures, Gumeniuk et al. (2008).

Extensive studies of the superconducting state in $PrOs_4Sb_{12}$, particularly when aided by an external magnetic field, revealed a fascinating crossover from the superconducting state to the high field-induced ordered phase taking place below 1.5 K and fields in the range between about 4.5T and 14T. The phase is also often referred to as the field-induced ordered phase, Aoki et al. (2002), Ho et al. (2002), and Kohgi et al. (2003). This momentous discovery stimulated even more intense efforts that led to a realization that $PrOs_4Sb_{12}$ is a unique chiral heavy fermion superconductor. Although the subsequently discovered superconductivity in the Pr-filled $[Pt_4Ge_{12}]$ framework shared similarities with $PrOs_4Sb_{12}$, namely, as the pair-breaking and time-reversal symmetry are concerned, the latter framework differed in one important aspect – the mass of the charge carriers was only mildly enhanced, lacking the status of heavy fermions typical in pnicogen-based skutterudites.

Filling the skutterudite voids also brings into play a variety of magnetic states, depending on the nature of the filler species and how the fillers interact with the neighboring ions of the framework, Sales (2003), Leithe-Jasper et al. (2004), and Yoshizawa et al. (2007). Understanding the magnetic state of skutterudites is not only of intrinsic interest, but it also reveals the nature of bonding and aids in illuminating the transport properties. One of the key issues is the crystalline electric field (CEF) potential of 12 surrounding pnicogen (or germanium in the case of APt_4Ge_{12} skutterudites) ions exerted on a filler located in the structural void of skutterudites. Although skutterudites are cubic structures, the void is a slightly distorted icosahedron, and this gives rise to non-spherical charge distribution around each filler. If the filler is a rare-earth element, the CEF splits the f-electron multiplet and results in what is referred to as a CEF energy scheme. Particularly relevant is the energy

separation between the ground state and the first excited state, which governs the magnetic and transport properties. How various fillers respond to the CEF (in other words, what kind of the CEF energy scheme develops) dictates the nature of magnetic interactions in the structure. Because the same filler in the voids of different skutterudites (altered frameworks) may have a very different CEF energy scheme, there are a myriad of unique magnetic phases observed in skutterudites.

Chapter 1 of the monograph starts with a brief review of the key features of the atomic structure and electronic bands of skutterudites. An extensive discussion of superconducting properties of the known superconducting skutterudites is presented in Chapter 2. Magnetic properties of skutterudites are covered in Chapter 3. The latter two chapters also include the basic aspects relevant to superconductivity and magnetism, respectively.

The target audiences of the book are researchers and graduate students working in the field of skutterudites who wish to have a broad understanding of the transport, superconducting, and magnetic properties of this exciting class of materials.

It is my distinct pleasure to acknowledge the work of my graduate students and postdocs, who worked with me during the past 25 years on the physical properties of skutterudites. I have also much enjoyed and benefitted from collaborations with numerous scientists, among them, Prof. Mercouri Kanatzidis, Prof. Pierre Ferdinand Poudeau, Prof. Xinfeng Tang, and Prof. Lidong Chen. I also want to acknowledge funding support for over 40 years extended to me by the US Federal Agencies and notably the US Department of Energy.

REFERENCES

Aoki, Y., T. Namiki, S. Ohsaki, S. R. Saha, H. Sugawara, and H. Sato, *J. Phys. Soc. Jpn.* **71**, 2098 (2002).

Bauer, E., N. A. Frederick, P.-C. Ho, V. S. Zapf, and M. B. Maple, *Phys. Rev. B* **65**, 100506(R) (2002).

Cheng, J.-G., J.-S. Zhou, K. Matsubayashi, P. P. Kong, Y. Kubo, Y. Kawamura, C. Sekine, C. Q. Jin, J. B. Goodenough, and Y. Uwatoko, *Phys. Rev. B* **88**, 024514 (2013).

DeLong, L. E. and G. P. Meisner, *Solid State Commun.* **53**, 119 (1985).

Gumeniuk, R., W. Schnelle, H. Rosner, M. Nicklas, A. Leithe-Jasper, and Y. Grin, *Phys. Rev. Lett.* **100**, 017002 (2008).

Ho, P.-C., V. S. Zapf, E. D. Bauer, N. A. Frederick, M. B. Maple, G. Giester, P. Rogl, S. T. Berger, C. H. Paul, and E. Bauer, *Int. J. Mod. Phys. B* **16**, 3008 (2002).

Jeitschko, W. and D. J. Braun, *Acta Crystallog.* **B33**, 3401 (1977).

Kohgi, M., K. Iwasa, M. Nakajima, N. Metoki, S. Araki, N. Bernhoeft, J. M. Mignot, A. Gukasov, H. Sato, Y. Aoki, and H. Sugawara, *J. Phys. Soc. Jpn.* **72**, 1002 (2003).

Leithe-Jasper, A., W. Schnelle, H. Rosner, M. Baenitz, A. Rabis, A. A. Gippius, E. N. Morozova, H. Borrmann, U. Burkhardt, R. Ramlau, U. Schwarz, J. A. Mydosh, Y. Grin, V. Ksenofontov, and S. Reiman, *Phys. Rev. B* **70**, 214418 (2004).

Maple, M. B., P.-C. Ho, V. S. Zapf, N. A. Frederick, E. D. Bauer, W. M. Yuhasz, F. M. Woodward, and J. W. Lynn, Proc. Int. Conf. Strongly Correlated Electrons with Orbital Degree of Freedom (ORBITAL 2001), *J. Phys. Soc. Jpn.* **71**, Suppl, 23 (2002).

Meisner, G. P., *Physica B&C* **108**, 763 (1981).

Sales, B. C., in *Handbook on the Physics and Chemistry of Rare Earths*, eds. K. A. Gschneidner, J.-C. Bunzli, and V. K. Pecharsky, Elsevier, Amsterdam, Vol. **33**, p.1 (2003).

Shirotani, I, S. Sato, C. Sekine, K. Takeda, I. Inagawa, and T. Yagi, *J. Phys.: Condens. Matter* **17**, 7353 (2005).

Uher, C., in *Thermoelectric Skutterudites*, CRC Press, Taylor & Francis Group, Boca Raton, FL, 2021.

Yoshizawa, M., Y. Nakanishi, T. Fujino, P. Sun, C. Sekine, and I. Shirotani, *J. Magn. Magn. Mater.* **310**, 1786 (2007).

About the Author

Ctirad Uher is a C. Wilbur Peters Professor of Physics at the University of Michigan in Ann Arbor.

He earned his BCs in physics with a University Medal from the University of New South Wales in Sydney, Australia. He carried out his graduate studies at the same institution under Professor H. J. Goldsmid on the topic of "Thermomagnetic effects in bismuth and its dilute alloys" and received his PhD in 1975. Subsequently, Professor Uher was awarded the prestigious Queen Elizabeth II Research Fellowship, which he spent at Commonwealth Scientific and Industrial Research Organization (CSIRO), National Measurement Laboratory (NML), in Sydney. He then accepted a postdoctoral position at Michigan State University, where he worked with Profs. W. P. Pratt, P. A. Schroeder, and J. Bass on transport properties at ultra-low temperatures.

Professor Uher started his academic career in 1980 as an assistant professor of Physics at the University of Michigan. He progressed through the ranks and became a full professor in 1989. The same year, the University of New South Wales awarded him the title of DSc for his work on the transport properties of semimetals. At the University of Michigan, he served as an associate chair of the Department of Physics and subsequently as an associate dean for research at the College of Literature, Sciences and Arts. In 1994, he was appointed as chair of physics, the post he held for the next ten years.

Professor Uher's 46 years of research is described in more than 530 refereed publications in the areas of transport properties of solids, superconductivity, diluted magnetic semiconductors, and thermoelectricity, and his h-index currently stands at 88 (Web of Science). He has written a number of authoritative review articles and has presented his research at numerous national and international conferences as an invited and plenary speaker. In 1996, he was elected fellow of the American Physical Society. Professor Uher was honored with the title of Doctor Honoris Causa by the University of Pardubice in the Czech Republic in 2002, and in 2010 he was awarded a named professorship at the University of Michigan. He received the prestigious China Friendship Award in 2011. Professor Uher supervised 17 PhD thesis projects and mentored numerous postdoctoral researchers, many of whom are leading scientists in academia and research institutions all over the world.

Professor Uher served on the Board of Directors of the International Thermoelectric Society. In 2004–2005, he was elected vice-president of the International Thermoelectric Society, and during 2006–2008, he served as its president.

1 Brief Review of the Structure and Electronic Bands in Skutterudites

1.1 INTRODUCTION

Skutterudites have a long history in the annals of science. The word skutterudite was first used by Wilhelm Karl von Haidinger (1845) to describe minerals of composition (Co, Ni, and Fe)As_3 that were mined in a small town called Skuterud in Norway. However, this class of minerals was known well before the time of von Haidinger under various names spanning from cobaltum eineraceum, the name given to it in 1529 by Georgius Agricola, fondly known as the father of mineralogy, to a simple Arsenikkobalt, the name coined by Gustav Rose (1852). Other synonyms occasionally encountered in the literature are modumite, smaltite, kieftite (referring specifically to $CoSb_3$), and chloanthite (for Ni-rich forms of the structure).

As accessory minerals of hydrothermal origin, they are found in many regions of the world usually accompanied by other Ni-Co minerals. The current description given by the International Mineralogical Association distinguishes four main groups of the mineral: skutterudites ($CoAs_{3-x}$), nickelskutterudites ($NiAs_{3-x}$), ferroskutterudites ((Fe-Co)As_3), and kieftite ($CoSb_3$). As recently pointed out by Schumer et al. (2017), because neither the mineral nor synthetic form of $NiAs_3$ exists, the nickelskutterudite group should properly be classified as (Ni, Co, and Fe)As_3.

One of the first synthetic forms of skutterudites was prepared by Jolibois (1910), who made single crystals from Sn flux; variants of this technique (Sb instead of Sn) have been used even today. Considering that the crystal structure and the phase diagram were not known at that time, Jolibois had to be a quite skilled researcher.

Appropriate structural characterization of synthetic skutterudites was performed by Ivar Oftedal (1928), who identified skutterudites to possess a body-centered cubic lattice belonging to the space group $Im\bar{3}$.

The scientific interest in skutterudites has been driven primarily by two phenomena: the fascinating and exotic superconducting properties of filled skutterudites and the prospect that by filling the structural void of the skutterudite lattice, the thermal conductivity can be dramatically reduced, making such filled skutterudites outstanding thermoelectric materials for power generation. The latter aspect, the development and properties of skutterudites as viable thermoelectric materials, has been extensively described in my recent book titled *Thermoelectric Skutterudites*, published by Taylor & Francis, Uher (2021). In the present monograph, the focus is on a plethora of fascinating magnetic properties and on the truly exotic nature of superconductivity observed in several filled skutterudites. However, to aid in an understanding of magnetic and superconducting properties of skutterudites, it is necessary to consider structural aspects and electronic bands of skutterudites. Thus, here the essential features of the crystalline lattice of skutterudites and the structure of their electronic bands are included. A detailed account of the above two aspects in given in the aforementioned monograph *Thermoelectric Skutterudites*.

In general, skutterudites can be divided into three main categories: binary skutterudites, ternary skutterudites, and filled skutterudites, and they are briefly reviewed in turn.

DOI: 10.1201/9781003225898-1

1.2 BINARY SKUTTERUDITES

As the term binary implies, the structure consists of two elements, and its general formula is MX_3, where M stands for an element of the column-9 transition metals Co, Rh, or Ir, and X represents a pnicogen (also pnictogen or pnictide) element P, As, or Sb. Thus, there are nine possible combinations constituting structurally stable bulk binary skutterudites. Occasionally, one finds reports of a stable form of NiP_3, Jolibois (1910), Biltz and Heimbrecht (1938), and Rundqvist and Larsson (1959). Because it is a thin film, it is possible to synthesize also metastable $FeSb_3$ (Daniel et al. 2015).

The arrangement of atoms in the crystalline lattice is depicted in Figure 1.1, where the left-hand side panel shows the unit cell with the transition metal atoms M occupying 8c (¼, ¼, ¼) sites (Wyckoff notation) that are octahedrally coordinated by pnicogen atoms at 24 g (0, *y*, *z*) sites, where *y* and *z* are the positional parameters that specify the exact location of a pnicogen atom. Typical of the skutterudite structure is the tilt of the MX_6 octahedrons, which gives rise to two large structural voids in the unit cell at position 2a (0, 0, 0) and leads to the formation of near-square pnicogen rings. The panel on the right-hand side of Figure 1.1 shows the unit cell shifted by one-quarter distance along the body diagonal. In this view, the transition metal atoms M form a simple cubic sublattice, and the near-square planar pnicogen rings are clearly depicted. There are six such pnicogen rings in the unit cell. Two of the eight small cubes do not contain the pnicogen rings and are locations of the two structural voids mentioned above. The chemical formula describing the unit cell of binary skutterudites is $\square_2M_8[X_4]_6 = 2(\square M_4[X_4]_3) = 2(\square M_4X_{12})$, where the empty square $\square$ stands for a structural void. It is customary to take just one-half of the unit cell, i.e., $\square M_4X_{12}$, the structure that has a valence electron count (VEC) of 72. The complete specification of binary skutterudites is given by the lattice parameter *a* accompanied by the positional parameters *y* and *z*.

The original structural analysis of skutterudites by Oftedal (1928) assumed a square planar configuration of the pnicogen rings, resulting in the so-called Oftedal relation

$$2\left(y+z\right)=1. \tag{1.1}$$

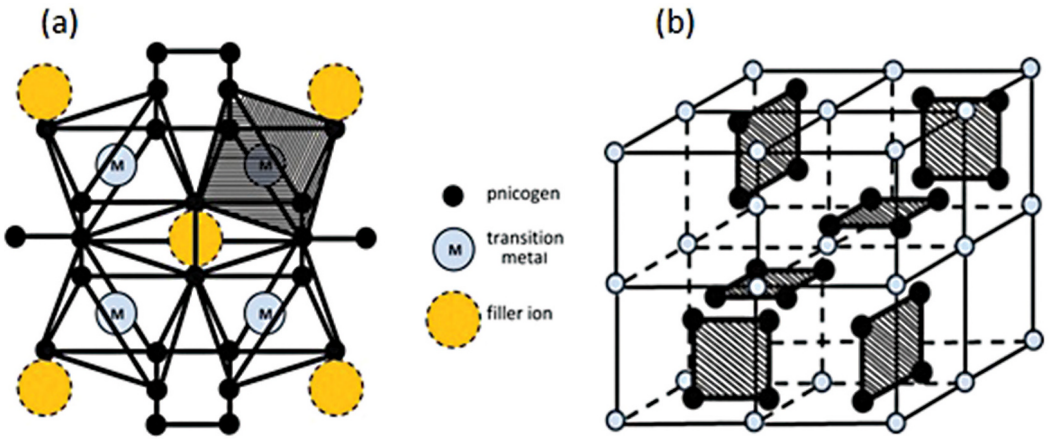

FIGURE 1.1 (a) Atomic arrangement in the unit cell of a binary skutterudite centered over a void at (0, 0, 0). The picture highlights the octahedral coordination of transition metals by pnicogen atoms and the tilt of the MX_6 octahedrons leading to the formation of two structural voids and four-membered pnicogen rings. (b) The unit cell of a binary skutterudite shifted by one-quarter distance along the body diagonal depicting the four-membered pnicogen rings that occupy six of the eight small cubes. The front upper left cube and the back bottom right cube do not contain pnicogen rings and are sites of two structural voids, often called cages.

More precise structural measurements performed by Kjekshus and Rakke (1974) revealed that the sides of the pnicogen rings are not equal, and all binary skutterudites possess rectangular rather than square planar ring configurations.

Binary skutterudites (except for NiP_3 and $FeSb_3$) are diamagnetic semiconductors. This follows from the mostly covalent nature of bonding and the fact that there are no unpaired electrons in the structure. Pnicogen atoms with their ns^2np^3 valence electron configuration use two electrons to form bonds with their two nearest neighbors on the pnicogen ring and three electrons to bond with two nearest transition metal atoms. Of the nine valence electrons of a transition metal atom of column 9, three electrons are used to establish bonds with the six neighboring pnicogen atoms, giving rise to octahedral d^2sp^3 hybrid orbitals, and the remaining six non-bonding electrons adopt a maximum spin-pairing d^6 configuration with zero spin. Structural parameters of binary skutterudites, including the void radius, are given in the monograph by Uher (2021).

While no bulk binary skutterudites form with the transition elements of columns 8 and 10 of the periodic table, (except for the already noted NiP_3), it is possible to partly replace Co, Rh, and Ir with their immediate transition metal neighbors Ni and Fe, Ru and Pd, and Os and Pt, respectively. Of course, such partial replacements alter the VEC and lead to a metallic behavior and paramagnetism. The solid solution limits in antimony skutterudites were established by Dudkin and Abrikosov (1957) and in arsenide skutterudites by Pleass and Heyding (1962). Roseboom (1962) pointed out that it is possible to make a coupled replacement of two Co atoms by one Fe and one Ni according to the equation

$$2Co^{3+}\left(d^6\right) \rightleftarrows Fe^{2+}\left(d^6\right) + Ni^{4+}\left(d^6\right). \tag{1.2}$$

Structures with symmetrically replaced Co preserve the total number of electrons, and all transition metal ions are in the low-spin d^6 configuration. This was, indeed, confirmed for arsenides by magnetic measurements performed by Nickel (1969), and Jeitschko et al. (2000) observed the same for phosphides.

Solid solubility limits for various families of skutterudites have been extensively explored. Lutz and Kliche (1981) established that phosphide and arsenide skutterudites form a complete series of solid solutions obeying Vegard's law. Unfortunately, solid solutions $MAs_{3-x}Sb_x$ between arsenides and antimonides are more restricted, and a miscibility gap exists for $0.4 < x < 2.8$. Solid solutions on the transition metal site were explored by Borshchevsky et al. (1995) with the emphasis on $Co_xIr_{1-x}Sb_3$, where a miscibility gap was observed in the range of $0.2 < x < 0.65$. Slack and Tsoukala (1994) were able to prepare $Rh_{0.5}Ir_{0.5}Sb_3$, but the full range of solubility was not explored. In $Rh_xCo_{1-x}Sb_3$, Wojciechowski (2007) observed a linear dependence of the cell parameter for all contents x, suggesting that solid solutions are unrestricted.

Binary skutterudites contain intrinsic defects that play an important role in the transport properties. The presence of intrinsic defects should not be surprising given that binary skutterudites are composed of rather high-melting-point transition metals and low-melting-point pnicogen species that have a high vapor pressure. The loss of pnicogen atoms during the synthesis is thus highly probable. However, energetically it is not favorable to create a pnicogen vacancy because this means severing a strong bond holding together the X_4 ring. Rather, it is Co interstitials and interstitial pairs that have the lowest formation energy and are therefore the dominant defects. Detailed accounts of defect formation, the temperature evolution of defects, and their strong effect on the charge carrier transport were extensively evaluated by Park and Kim (2010) and by Li et al. (2016).

Realistic band structure calculations must reflect the key structural aspects of skutterudites, namely, the existence of the near-square pnicogen rings, the octahedral coordination of transition metals by pnicogen atoms, and the fact that pure binary skutterudites are diamagnetic semiconductors. Although there were early attempts to elucidate the structure of electronic bands in binary skutterudites, Jung et al. (1990), real advances had to wait until the algorithms for first-principles

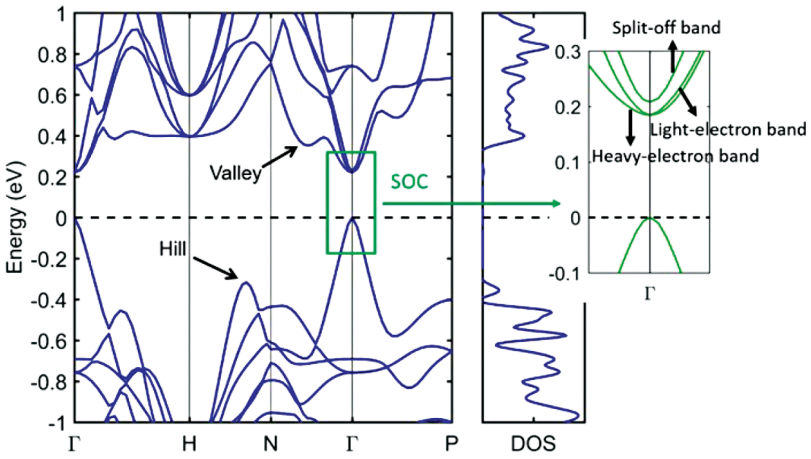

FIGURE 1.2 The band structure and the density-of-states of $CoSb_3$ around the Fermi energy. Of interest is a "valley" band some 0.13 eV above the triply degenerate conduction band at Γ. The inset on the right shows the conduction band calculated under the influence of split-orbit coupling. Reproduced from C. Z. Hu et al., *Physical Review B* 95, 165204 (2017). With permission from the American Physical Society.

calculations became robust enough to capture the complexity of the atomic structure of skutterudites, including their rather open environment. In the first such study, Singh and Pickett (1994) have shown that binary skutterudites possess a considerable indirect pseudogap around the Fermi level, which is crossed by a single linearly dispersing band that touches (nearly so in $CoSb_3$) the conduction band at Γ. With the improvements of functionals used in density functional theory (DFT) calculations, subsequent numerous treatments sharpened the position of the bands in various binary skutterudites and revealed their detailed features. The reader might find useful articles by Llunell et al. (1996), Sofo and Mahan (1999), Fornari and Singh (1999), Lefebvre-Devos et al. (2001), Takegahara and Harima (2003a), Kurmaev et al. (2004), Chaput et al. (2005), Wei et al. (2009), Smith et al. (2011), Pardo et al. (2012), Hammerschmidt et al. (2013), Nieroda et al. (2013), Khan et al. (2015), Tang et al. (2015), Hu et al. (2017), Kolezynski and Szczypka (2017), Yang et al. (2019), and Isaacs and Wolverton (2019).

Of the plethora of band structure calculations, two studies are of particular interest. Tang et al. (2015) drew attention to the importance of multi-valley bands in binary skutterudites, where the Γ-point conduction band in $CoSb_3$ is triply degenerate and one of the bands develops a higher-lying minimum along the Γ-N direction. The minimum is strongly temperature-dependent, moves down in energy as the temperature increases, and converges with the Γ-point bands at about 700 K. Subsequent band structure calculations of $CoSb_3$ by Hu et al. (2017) are depicted in Figure 1.2. Another interesting feature of the skutterudite band structure was pointed out by Smith et al. (2011) and expanded by Pardo et al. (2012). They considered the formation of the band gap as the structure evolves from a highly metallic perovskite to a semiconducting skutterudite and have shown that $CoSb_3$ is very near a conventional-to-topological transition. With a small tetragonal strain and spin-orbit coupling, $CoSb_3$ was predicted to become a topological insulator phase.

1.3 TERNARY SKUTTERUDITES

Ternary skutterudites are synthetically modified binary skutterudites where isoelectronic substitutions are made either on the cation site M by a pair of elements from columns 8 and 10 or on the pnicogen site with a pair of elements from columns 14 and 16. An example of the former is $Fe_{0.5}Ni_{0.5}Co_3$, Kjekshus and Rakke (1974), and that of the latter is $CoGe_{1.5}Se_{1.5}$, Korenstein et al.

(1977). The primary interest in ternary skutterudites was driven by a possibility of significantly lowering the lattice thermal conductivity, hoping that it would make the structure more suitable for thermoelectric applications. Unfortunately, a concomitant strong degradation of the electrical conductivity was a major impediment, and no ternary skutterudites have emerged as truly promising thermoelectric materials. While some structural modifications (distortion of the ring structure, deviation of the dihedral angle from the original 90°, and even lowering of the symmetry) take place because of substitutions, particularly when they are conducted on the pnicogen site where they distort the four-membered pnicogen rings, Lyons et al. (1978), Lutz and Kliche (1981), Partik et al. (1996), Fleurial et al. (1997), Vaqueiro et al. (2006), Volja et al. (2012), and Zevalkink et al. (2015), the isoelectronic nature of substitutions leaves the VEC unchanged and the undoped ternary skutterudites offer no special interest for magnetic studies as they remain diamagnetic materials. Moreover, detailed structural measurements performed by Vaqueiro et al. (2008) revealed that many ternary skutterudites formed by a substitution on the pnicogen site, including $IrGe_{1.5}S_{1.5}$ and $RhSn_{1.5}Te_{1.5}$, often described as single phase structures, in reality contain some 10% of IrGe and $RhTe_2$, respectively.

Changes in the electronic band structure of ternary skutterudites were first investigated by Bertini and Cenedese (2007) in $CoSn_{1.5}Te_{1.5}$ and indicated some 22% reduction in the band gap compared to $CoSb_3$. Moreover, the authors noted a significant charge transfer, which suggested a stronger ionicity of the bonds. Subsequent detailed DFT calculations by Volja et al. (2012) on several ternary skutterudites revealed significantly larger rather than smaller band gaps due to the more ionic bonding. The single band emerging from the valence band manifold toward the Γ point conduction band was preserved, but its linear dispersion was weaker. The study by Zevalkink et al. (2015) agreed substantially with the findings of Volja et al. A comparison of band structures of alkali earth-filled ternary skutterudites with the unfilled forms of the structure was made using DFT calculations by Bang et al. (2016). The study was aimed at improving the thermoelectric properties, but the outcome was uncertain because the exact degree of degradation of the thermal conductivity could not be determined based on the analysis of phonon dispersion only.

1.4 FILLED SKUTTERUDITES

As noted in Section 1.1, the tilt of the MX_6 octahedrons creates large icosahedral voids at the 2a sites in the skutterudite structure. The voids are large enough to accommodate a large variety of ions of alkali, alkaline, and rare earth species as well as elements, such as Li, Tl, Sn, In, and Ga. Filling of the voids was demonstrated first by Jeitschko and Braun (1977) with phosphide-based skutterudites and soon after replicated with antimonides and arsenides, Braun and Jeitschko (1980a and 1980b). Skutterudites with the 2a sites occupied are referred to as filled skutterudites.

If not for two rather unrelated findings, skutterudites would likely be an interesting open structure compound but mostly inconsequential as far as prominent physical properties and practical potential are concerned. The first momentous event was the discovery of superconductivity in $LaFe_4P_{12}$, Meisner (1981), with a rather high transition temperature of 4.1 K in a structure that contained Fe, the element that typically breaks the Cooper pairs. The discovery opened the door to intensive worldwide efforts to explore other filled skutterudites, which culminated with revealing $PrOs_4Sb_{12}$ as a truly exotic heavy fermion superconductor, Maple et al. (2002) and Bauer et al. (2002). The present monograph is dedicated to the superconducting and magnetic properties of filled skutterudites. The other important milestone was the idea of Slack and Tsoukala (1994) and Slack (1995) that filling the voids of the skutterudite structure might make skutterudites an example of the phonon-glass electron-crystal material that maintains the outstanding electronic properties of binary skutterudites, while its thermal conductivity is drastically degraded by vibrations of loosely bonded filler species. Thermal conductivity measurements of filled skutterudites confirmed the exceptionally low values of the thermal conductivity, Morelli and Meisner (1995), Fleurial et al. (1996), Sales et al. (1996), Tritt et al. (1996), and Nolas et al. (1996), and since then, filled skutterudites have become one of

the most intensely studied thermoelectric materials intended for power generation applications. The properties and the development of skutterudites as promising thermoelectric materials are described in a book by Uher (2021).

The presence of a filler alters the structural parameters, Chakoumakos and Sales (2006), typified by an increased lattice constant a and an unequal rise in the positional parameters y and z that makes the pnicogen ring structure more square as the filling increases. Filled skutterudites can be categorized into several groups, depending on the framework they are made of.

1.4.1 Filled Skutterudites with the $[M_4X_{12}]$ Framework

The $[M_4X_{12}]$ framework is isoelectronic with that of the binary skutterudites, and skutterudites of the form $R_yM_4X_{12}$ can be filled only partially, i.e., $y < 1$, with electropositive fillers R. As the electrons of the filler R are stripped off and donated to the structure, filled skutterudites $R_yM_4X_{12}$ are invariably n-type conductors. The filling fraction y is a strong function of the valence state of the filler with trivalent rare earth ions having a particularly low filling fraction. Moreover, due to the lanthanide contraction, the smaller and heavier rare earth fillers beyond Sm are too small to be trapped in the large skutterudite voids. Divalent Eu or intermittent valence Yb and all alkaline earth fillers have a significantly higher filling limit up to 45%. Alkali ions, particularly Na and K, can fill over 60% of voids in $CoSb_3$. Theoretical criteria for filling were developed by Chen (2002), and a particularly useful form was presented by Shi et al. (2005). Making use of high pressure during the synthesis, it is possible to fill the voids with even smaller and heavier rare earth fillers, including Lu, Sekine et al. (1998 and 2000) and Shirotani et al. (2003), and enhance the filling fraction of many fillers, Takizawa et al. (2002) and Tanaka et al. (2007).

Reports on the band structure of filled skutterudites that have an electrically neutral $[M_4X_{12}]$ framework are few. The first one was by Akai et al. (2002), who considered Yb-filled $CoSb_3$, but the calculations were made for an unrealistic case of 100% Yb filling. A large family of new filled skutterudites based on the column-9 transition metals (Co, Rh, and Ir) was revealed by Luo et al. (2015) who strictly adhered to the Zintl concept in their band structure calculations and confirmed their findings by synthesizing the structures. In general, the filled $[M_4X_{12}]$ framework does not support superconductivity. However, when the filler content is dramatically enhanced by applying high pressure during the synthesis, as shown by Shirotani et al. (2005) in the case of $La_{0.6}Rh_4P_{12}$ and by Imai et al. (2007) with $La_{0.8}Rh_4P_{12}$, the transition temperature attains the record-high values among all skutterudites of 17 K and 14.9 K, respectively. A similar approach, this time with a very high content of Ba fillers in the Ir-based phosphide and arsenide skutterudites (supported by DFT calculations of the density-of-states), led to a superconducting transition temperature of 5.6 K for $Ba_{0.89}Ir_4P_{12}$ and 4.8 K for $Ba_{0.85}Ir_4As_{12}$, Qi et al. (2017).

1.4.2 Filled Skutterudites with the $[T_4X_{12}]^{4-}$ Framework

When one speaks of filled skutterudites, it is generally understood that the structure contains the $[T_4X_{12}]^{4-}$ framework rather than the neutral $[M_4X_{12}]$ framework. The difference is in the transition metal that is now a Fe-like column-8 element (Fe, Ru, and Os), which makes the framework deficient of four electrons. The role of the filler ion R is to supply the missing electrons, saturate the bond, and electrically neutralize the structure. This requires a tetravalent filler ion R^{4+}, which would bring the VEC to 72. In reality, this is plausible only with Th and U. All other fillers, including Ce, assumed originally by Jeitschko and Braun (1977) to be tetravalent, cannot supply four electrons. The VEC of the fully filled skutterudites will then be less than 72, and the structure will be a paramagnetic metal, unless magnetic interactions set in at lower temperatures or the structure becomes a superconductor. It is possible to bring the structure back into its semiconducting regime (and the VEC of 72) by charge compensation. This means replacing some pnicogen atoms in the

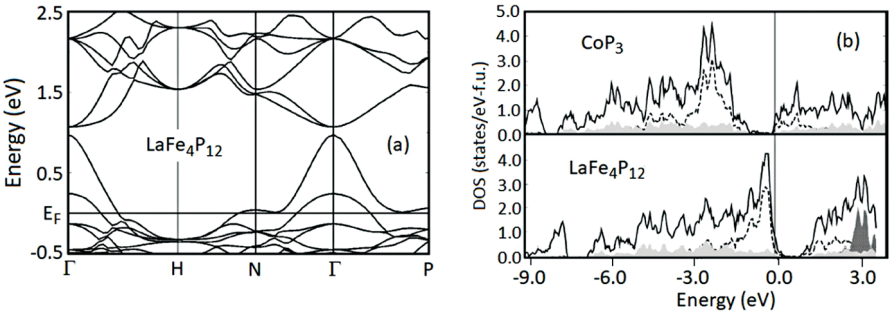

FIGURE 1.3 (a) Band structure of $LaFe_4P_{12}$ near the Fermi level. (b) Density-of-states of $LaFe_4P_{12}$ compared to the density-of-states of CoP_3. The solid lines are the total density-of-states, the dashed lines indicate the contribution of Co-d states, the light gray regions designate the phosphorus p states, and the dark gray region represents the resonant La f-component. Adapted from M. Fornari and D. J. Singh, *Physical Review B* 59, 9722 (1999). With permission from the American Physical Society.

24g positions with elements from column 14 (e.g., Ge or Sn) or replacing a fraction of the Fe-like element at 8c sites by a Co-like transition metal. Making such substitutions in the spirit of the Zintl concept greatly enhances the family of skutterudites and gives rise to an abundance of fascinating physical properties.

In 1981, Meisner discovered superconductivity in $LaFe_4P_{12}$. This surprising observation was soon followed by the discovery of superconductivity in several other phosphide skutterudites. It is not surprising that then phosphide skutterudites became the primary target of band structure studies, hoping to shed light on the mechanism of superconductivity. The first among many studies were DFT calculations performed by Nordström and Singh (1996). The calculations revealed a greater complexity of the electronic bands due to the presence of a filler and indicated heavy electron masses associated with the flat conduction bands and a tendency of the pnicogen rings becoming more square upon filling. As an example of the electronic band structure of filled skutterudites, Figure 1.3 depicts the electronic bands in $LaFe_4P_{12}$ near the Fermi level as well as the density-of-states of $LaFe_4P_{12}$ compared to the density-of-states of binary CoP_3.

Band structure calculations have been performed for many different filled skutterudites, and to aid interested readers, the targeted filled skutterudite is indicated in the following references: Singh and Mazin (1997), Singh (2002), Takegahara and Harima (2002) [$LaFe_4Sb_{12}$]; Harima (1998) [$LaFe_4P_{12}$]; Harima and Takegahara (2003a) [$LaFe_4X_{12}$, X = P, As, and Sb]; Harima and Takegahara (2003b) [$PrRu_4P_{12}$, $PrFe_4P_{12}$, and $LaFe_4P_{12}$]; Saha et al. (2002), Harima (2008) [$LaRu_4P_{12}$]; Harima and Takegahara (2002a), Harima et al. (2002) [perfect nesting in $PrRu_4P_{12}$]; Harima and Takegahara (2002b) [$LaOs_4Sb_{12}$]; Akai et al. (2002), Takegahara and Harima (2002) [$YbCo_4Sb_{12}$ and $YbFe_4Sb_{12}$]; H. Sugawara et al. (2002), Harima and Takegahara (2005) [$PrOs_4Sb_{12}$]; Takegahara and Harima (2003b) [$ThFe_4P_{12}$]; Takegahara and Harima (2008) [$SmOs_4Sb_{12}$]; Yan et al. (2012) [$CeOs_4As_{12}$ and $CeOs_4Sb_{12}$]; Nieroda et al. (2013) [$Ag_xCo_4Sb_{12}$]; Ram et al. (2014) [$LaRu_4X_{12}$, X = P, As, and Sb]; Xing et al. (2015) [$LaFe_4X_{12}$ and $NaFe_4X_{12}$, X = P, As, and Sb]; Luo et al. (2015) [$LaT_4Sb_9Sn_3$]; Shankar et al. (2017) [$EuRu_4As_{12}$]; Hu et al. (2017) [$La_xCo_4Sb_{12}$]; Qi et al. (2017) [$Ba_xIr_4As_{12}$]; and Tütüncü et al. (2017) [$LaRu_4P_{12}$ and $LaRu_4As_{12}$].

1.4.3 Filled Skutterudites with the $[Pt_4Ge_{12}]$ Framework

Skutterudites with an entirely new polyanionic framework based on $[Pt_4Ge_{12}]$ were reported by Bauer et al. (2007) and Gumeniuk et al. (2008a). Although the voids in this structure are somewhat smaller than those in $CoSb_3$, all other structural aspects are essentially identical to those of the

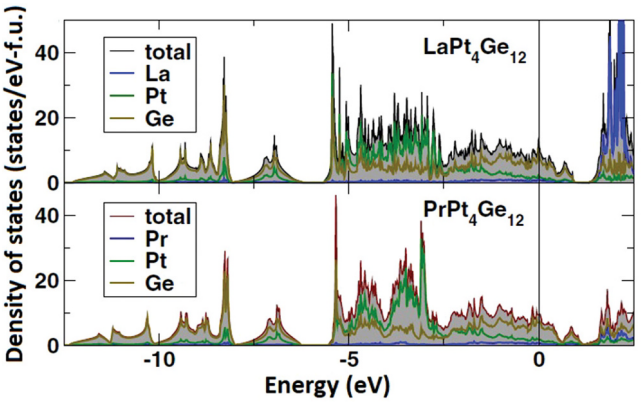

FIGURE 1.4 Total and atom-resolved electronic density-of-states for $LaPt_4Ge_{12}$ and $PrPt_4Ge_{12}$. Modified from R. Gumeniuk et al., *Physical Review Letters* 100, 017002 (2008). With permission from the American Physical Society.

pnicogen-based skutterudites. The filler species here transfer the charge to the polyanion and in the process stabilize the structure. Although not contemplated for use as thermoelectric materials (Pt and Ge are far too expensive), the filled forms of the $[Pt_4Ge_{12}]$ framework display equally exciting magnetic and superconducting properties as do their pnicogen-based structural relatives.

The first reports of the existence and properties of skutterudites with the $[Pt_4Ge_{12}]$ framework were accompanied by DFT calculations of the electronic bands and contributions of the respective constituting elements to the density-of-states, Bauer et al. (2007), Gumeniuk et al. (2008a), Grytsiv et al. (2008), and Tran et al. (2009a, 2009b). The most notable feature distinguishing $[Pt_4Ge_{12}]$-based skutteruddites from pnicogen-based skutterudites is the overwhelming dominance of Ge p states in the density-of-states near the Fermi energy. This suggests that the dominant role in the physical properties, such as superconductivity, is played by the $[Pt_4Ge_{12}]$ framework and the fillers have only a minor effect. The results also indicated a substantial electron transfer from the fillers to Pt that helps to stabilize the structure. An example of the computed density-of-states of skutterudites with the $[Pt_4Ge_{12}]$ framework is shown in Figure 1.4 for $LaPt_4Ge_{12}$ and $PrPt_4Ge_{12}$.

Band structure calculations devoted to skutterudites with the $[Pt_4Ge_{12}]$-based framework and filled with a specific filler can be found in the following publications: Bauer et al. (2007, 2008a), Grytsiv et al. (2008), Khan et al. (2008) $[BaPt_4Ge_{12}]$; Bauer et al. (2007), Gumeniuk et al. (2008b), Rosner et al. (2009), Khan et al. (2008) $[SrPt_4Ge_{12}]$; Gumeniuk et al. (2008a), Humer et al. (2013), Tűtűncű et al. (2017) $[LaPt_4Ge_{12}]$; Nicklas et al. (2012) $[CePt_4Ge_{12}]$; Gumeniuk et al. (2010) $[SmPt_4Ge_{12}]$; Gumeniuk et al. (2008a) $[PrPt_4Ge_{12}]$; Bauer et al. (2008b), Tran et al. (2009a, 2009b), Galvan (2009) $[ThPt_4Ge_{12}]$; and Bauer et al. (2008b) $[UPt_4Ge_{12}]$.

1.4.4 Filled Skutterudites with Electronegative Fillers

The stability of all forms of filled skutterudites discussed above relied on the transfer of electrons to the framework. It thus came as a great surprise when Fukuoka and Yamanaka (2010) reported that using a high-pressure synthesis they filled $RhSb_3$ with iodine and the filler attained the valence state 1−, i.e., iodine acted as an acceptor. The discovery of an anion-filled skutterudite led to more studies. Li et al. (2014) documented that iodine can also be trapped as an electronegative filler in $CoSb_3$, and Zhang et al. (2015) showed the same for the compensated $Fe_4Co_{4-x}Sb_{12}$ framework. Reports of other halides as electronegative fillers were soon followed by reports of Ortiz et al. (2016) filling bromine into $CoSb_3$ and Duan et al. (2016) inserting chlorine into the same framework. By replacing

a fraction of Sb with Te, Wang et al. (2018) were able to insert sulfur as an electronegative filler into $CoSb_3$, and Wan et al. (2018) and Li et al. (2019) achieved the same feat by substituting a small amount of Pd for Co and Ni for Co, respectively. Without doping electrons at the site of Sb or partly replacing Co with transition metals of column 10, the filling fraction limit of sulfur in $CoSb_3$ is only about 5%, Ghosh et al. (2020). Theoretical analysis of filling with sulfur and doping with Ni, Pd, and Pt at the site of Co was performed by Tu et al. (2019). Se is a particularly interesting electronegative filler because it plays a dual role, it fills the voids of $CoSb_3$ and also substitutes at the sites of Sb where it charge compensates the presence of Se in the voids. Additional electrons can be introduced by replacing a fraction of Co with, e.g., Pd, Bao et al. (2019).

With this brief summary of structural features and electronic bands of skutterudites, we now turn to the superconducting and magnetic properties of skutterudite compounds.

REFERENCES

Akai, K., K. Koga, K. Oshiro, and M. Matsuura, *Proc. 20th Int. Conf. on Thermoelectrics*, IEEE Catalog Number 01TH8589, Piscataway, NJ, p. 93 (2002).

Bang, S., D.-H. Wee, A. Li, M. Fornari, and B. Kozinsky, *J. Appl. Phys.* **119**, 205102 (2016).

Bao, X., Z. H. Wu, and H. Q. Xie, *Mater. Res. Express* **6**, 025511 (2019).

Bauer, E., N. A. Frederick, P.-C. Ho, V. S. Zapf, and M. B. Maple, *Phys. Rev. B* **65**, 100506(R) (2002).

Bauer, E., A. Grytsiv, X.-Q. Chen, N. Melnychenko-Koblyuk, G. Hilscher, H. Kaldarar, H. Michor, E. Royanian, G. Giester, M. Rotter, R. Podloucky, and P. Rogl, *Phys. Rev. Lett.* **99**, 217001 (2007).

Bauer, E., A. Grytsiv, X.-Q. Chen, N. Melnychenko-Koblyuk, G. Hilscher, H. Kaldarar, H. Michor, E. Royanian, M. Rotter, R. Podloucky, and P. Rogl, *Adv. Mater.* **20**, 1325 (2008a).

Bauer, E., X.-Q. Chen, P. Rogl, G. Hilscher, H. Michor, E. Royanian, R. Podloucky, G. Giester, O. Sologub, and A. P. Goncalves, *Phys. Rev. B* **78**, 064516 (2008b).

Bertini, L. and S. Cenedese, *Phys. Stat. Solidi (RRL)* **1**, 244 (2007).

Biltz, W. and M. Heimbrecht, *Z. Anorg. Allg. Chem.* **237**, 132 (1938).

Borshchevsky, A., J.-P. Fleurial, E. Allevato, and T. Caillat, *Proc. 13th Int. Conf. on Thermoelectrics*, American Institute of Physics, Kansas City, p. 3 (1995).

Braun, D. J. and W. Jeitschko, *J. Less-Common Met.* **72**, 147 (1980a).

Braun, D. J. and W. Jeitschko, *J. Solid State Chem.* **32**, 357 (1980b).

Chakoumakos, B. C. and B. C. Sales, *J. Alloys and Compd.* **407**, 87 (2006).

Chaput, L., P. Pecheur, J. Tobola, and H. Scherrer, *Phys. Rev. B* **72**, 085126 (2005).

Chen, L. D., *Proc. 21st Int. Conf. on Thermoelectrics*, IEEE Catalog Number 02TH8657, Piscataway, NJ, p. 42 (2002).

Daniel, M. V., L. Hammerschmidt, C. Schmidt, F. Timmermann, J. Franke, N. Jöhrmann, M. Hietschold, D. C. Johnson, B. Paulus, and M. Albrecht, *Phys. Rev. B* **91**, 085410 (2015).

Duan, B., Jiong Yang, J. R. Salvador, Y. He, B. Zhao, S. Wang, P. Wei, F. S. Ohuchi, W. Q. Zhang, R. P. Hermann, O. Gourdon, S. X. Mao, Y. W. Cheng, C. M. Wang, J. Liu, P. C. Zhai, X. F. Tang, Q. J. Zhang, and Jihui Yang, *Energy & Environ. Sci.* **9**, 2090 (2016).

Dudkin, L. D. and N. K. Abrikosov, *Zh. Neorg. Khim.* **2**, 212 (1957).

Fleurial, J.-P., A. Borshchevsky, T. Caillat, D. T. Morelli, and G. P. Meisner, *Proc. 15th Int. Conf. on Thermoelectrics*, IEEE Catalog Number 96TH8169, Piscataway, NJ, p. 91 (1996).

Fleurial, J.-P., T. Caillat, and A. Borshchevsky, *Proc. 16th Int. Conf. on Thermoelectrics*, IEEE Catalog Number 97TH8291, Piscataway, NJ, p. 1 (1997).

Fornari, M. and D. J. Singh, *Phys. Rev. B* **59**, 7922 (1999).

Fukuoka, H. and S. Yamanaka, *Chem. Mater.* **22**, 47 (2010).

Galvan, G. H., *J. Supercond. Nov. Magn.* **22**, 367 (2009).

Ghosh, S., K. K. Raut, A. Ramaksishnan, K.-H. Chen, S.-J. Hong, and R. C. Mallik, *AIP Conf. Proc.* **2265**, 030606 (2020).

Grytsiv, A., X.-Q. Chen, N. Melnychenko-Koblyuk, P. Rogl, E. Bauer, G. Hilscher, H. Kaldarar, H. Michor, E. Royanian, R. Podloucky, M. Rotter, and G. Giester, *J. Phys. Soc. Jpn.* **77**, 121 (2008).

Gumeniuk, R., W. Schnelle, H. Rosner, M. Nicklas, A. Leithe-Jasper, and Y. Grin, *Phys. Rev. Lett.* **100**, 017002 (2008a).

Gumeniuk, R., H. Rosner, W. Schnelle, M. Nicklas, A. Leithe-Jasper, and Y. Grin, *Phys. Rev. B* **78**, 052504 (2008b).
Gumeniuk, R., M. Schöneich, A. Leithe-Jasper, W. Schnelle, M. Nicklas, H. Rosner, A. Ormeci, U. Burkhardt, M. Schmidt, U. Schwarz, M. Ruck, and Y. Grin, *New J. Phys.* **12**, 103035 (2010).
Haidinger, Wilhelm Karl, in *Handbuch der Bestimmenden Mineralogie*, Vienna (1845).
Hammerschmidt, L., S. Schlecht, and B. Paulus, *Phys. Stat. Solidi A* **210**, 131 (2013).
Harima, H., *J. Mag. Magn. Mater.* **177–181**, 321 (1998).
Harima, H., *J. Phys. Soc. Jpn.* **77**, 114 (2008).
Harima, H. and K. Takegahara, *Physica B* **312–313**, 843 (2002a).
Harima, H. and K. Takegahara, *Physica C* **388–389**, 555 (2002b).
Harima, H., K. Takegahara, K. Ueda, and S. H. Curnoe, *Acta Phys. Pol. B* **34**, 1189 (2002).
Harima, H. and K. Takegahara, *Physica B* **328**, 26 (2003a).
Harima, H. and K. Takegahara, *J. Phys.: Condens. Matter* **15**, S2081 (2003b).
Harima, H. and K. Takegahara, *Physica B* **359–361**, 920 (2005).
Hu, C. Z., X. Y. Zeng, Y. F. Liu, M. H. Zhou, H. J. Zhao, T. M. Tritt, J. He, J. Jakowski, P. R. C. Kent, J. S. Huang, and B. G. Sumpter, *Phys. Rev. B* **95**, 165204 (2017).
Humer, S., E. Royanian, H. Michor, E. Bauer, A. Grytsiv, M.-X. Chen, R. Podloucky, and P. Rogl, in *New Materials for Thermoelectric Applications: Theory and Experiment*, NATO Science for Peace and Security Series B: Physics and Biophysics, Springer Science, Dordrecht, p. 115 (2013).
Imai, M., M. Akaishi, and I. Shirotani, *Supercond. Sci. Technol.* **20**, 832 (2007).
Isaacs, E. B. and C. Wolverton, *Chem. Mater.* **31**, 6154 (2019).
Jeitschko, W. and D. J. Braun, *Acta Crystallogr. B* **33**, 3401 (1977).
Jeitschko, W., A. J. Foecker, D. Paschke, M. V. Dewalsky, E. B. H. Evers, B. Kűnnen, A. Lang, G. Kotzyba, U. C. Rodewald, and M. H. Möller, *Z. Anorg. Allg. Chem.* **626**, 1112 (2000).
Jolibois, P., *C. R. Acad. Sci.* **150**, 106 (1910).
Jung, D. W., M.-H. Whangbo, and S. Alvarez, *Inorg. Chem.* **29**, 2252 (1990).
Khan, B., H. A. Rahnamaye Aliabad, Saifullah, S. Jalali-Asadabadi, I. Khan, and I. Ahmad, *J. Alloys Compd.* **647**, 364 (2015).
Khan, R. T., E. Bauer, X.-Q. Chen, R. Podloucky, and P. Rogl, *J. Phys. Soc. Jpn.* **77**, 350 (2008).
Kjekshus, A. and T. Rakke, *Acta Chem. Scand., Ser. A* **28**, 99 (1974).
Kolezynski, A. and W. Szczypka, *J. Alloys Compd.* **691**, 299 (2017).
Korenstein, R., S. Soled, A. Wold, and G. Collin, *Inorg. Chem.* **16**, 2344 (1977).
Kurmaev, E. Z., A. Moewes, I. R. Shtein, L. D. Finkelstein, A. L. Ivanovski, and H. Anno, *J. Phys.: Condens. Matter* **16**, 979 (2004).
Lefebvre-Devos, I., M. Lassalle, X. Wallart, J. Olivier-Fourcade, L. Monconduit, and J. Jumas, *Phys. Rev. B* **63**, 125110 (2001).
Li, G.-D., S. Bajaj, U. Aydemir, S.-Q. Hao, H. Xiao, W. A. Goddard III, P. C. Zhai, Q.-J. Zhang, and G. J. Snyder, *Chem. Mater.* **28**, 2172 (2016).
Li, J. L., B. Duan, H. J. Yang, H. T. Wang, G. D. Li, J. Yang, G. Chen, and P. C. Zhai, *J. Mater. Chem. C* **7**, 8079 (2019).
Li, X.-D., B. Xu, L. Zhang, F.-F. Duan, X.-L. Yan, J.-Q. Yang, and Y.-J. Tian, *J. Alloys Compd.* **615**, 177 (2014).
Llunell, M., P. Alemany, S. Alvarez, V. P. Zhukov, and A. Vernes, *Phys. Rev. B* **53**, 10605 (1996).
Luo, H. X., J. W. Krizan, L. Muechler, N. Haldolaarachchige, T. Klimczuk, W. W. Xie, M. K. Fuccillo, C. Felser, and R. J. Cava, *Nat. Commun.* **6**, 6489 (2015).
Lutz, H. D. and G. Kliche, *J. Solid State Chem.* **40**, 64 (1981).
Lyons, A., R. P. Gruska, C. Case, S. N. Subbarao, and A. Wold, *Mater. Res. Bull.* **13**, 125 (1978).
Maple, M. B., P.-C. Ho, V. S. Zapf, N. A. Frederick, E. Bauer, W. M. Yuhasz, F. M. Woodward, and J. W. Lynn, *Proc. Int. Conf. on Strongly Correlated Electrons with Orbital Degrees of Freedom* (ORBITAL 2001), *J. Phys. Soc. Jpn.* **71**, 23 (2002).
Meisner, G. P., *Physica B* **108**, 763 (1981).
Morelli, D. T. and G. P. Meisner, *J. Appl. Phys.* **77**, 3777 (1995).
Nickel, E. H., *Chem. Geol.* **5**, 233 (1969).
Nicklas, M., S. Kirchner, R. Borth, R. Gumeniuk, W. Schnelle, H. Rosner, H. Borrmann, A. Leithe-Jasper, Y. Grin, and F. Steglich, *Phys. Rev. Lett.* **109**, 236405 (2012).
Nieroda, P., K. Kutorasinski, J. Tobola, and K. Wojciechowski, *J. Electron. Mater.* **43**, 1681 (2013).
Nolas, G. S., G. A. Slack, D. T. Morelli, T. M. Tritt, and A. C. Ehrlich, *J. Appl. Phys.* **79**, 4002 (1996).

Nordström, L. and D. J. Singh, *Phys. Rev. B* **53**, 1103 (1996).
Oftedal, I., *Z. Kristallogr.* **A66**, 517 (1928).
Ortiz, B. R., C. M. Crawford, R. W. McKinney, P. A. Parilla, and E. S. Toberer, *J. Mater. Chem. A* **4**, 8444 (2016).
Pardo, V., J. C. Smith, and W. E. Pickett, *Phys. Rev. B* **85**, 214531 (2012).
Park, C.-H. and Y.-S. Kim, *Phys. Rev. B* **81**, 085206 (2010).
Partik, M., C. Kringe, and H. D. Lutz, *Z. Kristallogr*. **211**, 304 (1996).
Pleass, C. M. and R. D. Heyding, *Canad. J. Chem.* **40**, 590 (1962).
Qi, Y. P., H. C. Lei, J. G. Guo, W. J. Shi, B. H. Yan, C. Felser, and H. Hosono, *J. Am. Chem. Soc.* **139**, 8106 (2017).
Ram, S., V. Kanchana, and M. C. Valsakumar, *J. Appl. Phys.* **115**, 093903 (2014).
Rose, G., in *Das Krystallo-Chemishe Mineralsystem*, Verlagen Wilhelm Engelmann, Leipzig, (1852).
Roseboom, E. H. Jr., *Am. Mineral.* **47**, 310 (1962).
Rosner, H. J., D. Gerger, D. Regesch, W. Schnelle, R. Gumeniuk, A. Leithe-Jasper, H. Fujiwara, T. Hauptricht, T. C. Koethe, H.-H. Hsieh, H.-J. Lin, C. T. Che, A. Ormeci, Y. Grin, and L. H. Tjeng, *Phys. Rev. B* **80**, 075114 (2009).
Rundqvist, S. and E. Larsson, *Acta Chem. Scand.* **13**, 551 (1959).
Saha, S. R., H. Sugawara, R. Sakai, Y. Aoki, H. Sato, Y. Inada, H. Shishido, R. Settai, Y. Onuki, and H. Harima, *Physica B* **328**, 68 (2002).
Sales, B. C., D. Mandrus, and R. K. Williams, *Science* **272**, 1325 (1996).
Schumer, B. N., M. B. Andrade, S. H. Evans, and R. T. Downs, *Am. Mineral.* **102**, 205 (2017).
Sekine, C., H. Saito, T. Uchiumi, A. Sakai, and I. Shirotani, *Solid State Commun.* **106**, 441 (1998).
Sekine, C., T. Uchiumi, I. Shirotani, K. Matsuhira, T. Sakakibara, T. Goto, and T. Yagi, *Phys. Rev. B* **62**, 11581 (2000).
Shankar, A., D. P. Rai, Sandeep, M. P. Ghimire, and R. K. Thapa, *Indian J. Phys.* **91**, 17 (2017).
Shi, X., W. Q. Zhang, L. D. Chen, and J. Yang, *Phys. Rev. Lett.* **95**, 185503 (2005).
Shirotani, I., Y. Shimaya, K. Kihou, C. Sekine, and T. Yagi, *J. Solid State Chem.* **174**, 32 (2003).
Shirotani, I., S. Sato, C. Sekine, K. Takeda, I. Inagawa, and T. Yagi, *J. Phys.: Condens. Matter* **17**, 7353 (2005).
Singh, D. J. and W. E. Pickett, *Phys. Rev. B* **50**, 11235 (1994).
Singh, D. J. and I. I. Mazin, *Phys. Rev. B* **56**, R1650 (1997).
Singh, D. J., *Mat. Res. Soc. Symp. Proc.* **691**, 15 (2002).
Slack, G. A., in *CRC Handbook of Thermoelectrics*, ed. D. M. Rowe, CRC Press, Boca Raton, FL, pp. 407–440 (1995).
Slack, G. A. and V. G. Tsoukala, *J. Appl. Phys.* **76**, 1665 (1994).
Sofo, J. O. and G. D. Mahan, *Mat. Res. Soc. Symp. Proc.* **545**, 315 (1999).
Smith, J. C., S. Banerjee, V. Pardo, and W. E. Pickett, *Phys. Rev. Lett.* **106**, 056401 (2011).
Sugawara, H., S. Osaki, S. R. Saha, Y. Aoki, H. Sato, Y. Inada, H. Shishido, R. Settai, Y. Onuki, H. Harima, and K. Oikawa, *Phys. Rev. B* **66**, 220504 (2002).
Takegahara, K. and H. Harima, *J. Phys. Soc. Jpn.* **71**, 240 (2002).
Takegahara, K. and H. Harima, *Physica B* **328**, 74 (2003a).
Takegahara, K. and H. Harima, *Physica B* **329–333**, 464 (2003b).
Takegahara, K. and H. Harima, *J. Phys. Soc. Jpn.* **77**, 193 (2008).
Takizawa, H., K. Okazaki, K. Uhedu, T. Endo, and G. S. Nolas, *Mater. Res. Soc. Symp. Proc.* **691**, 37 (2002).
Tanaka, K., Y. Kawahito, Y. Yonezawa, D. Kikuchi, H. Aoki, K. Kuwahara, M. Ichihara, H. Sugawara, Y. Aoki, and H. Sato, *J. Phys. Soc. Jpn*. **76**, 103704 (2007).
Tang, Y. L., Z. M. Gibbs, L. A. Agapito, G. Li, H.-S. Kim, M. B. Nardelli, S. Curtarolo, and G. J. Snyder, *Nat. Mater.* **14**, 1223 (2015).
Tran, V. H., D. Kaczorowski, W. Miller, and A. Jezirski, *Phys. Rev. B* **79**, 054520 (2009a).
Tran, V. H., B. Nowak, A. Jezirski, and D. Kaczorowski, *Phys. Rev. B* **79**, 144510 (2009b).
Tritt, T. M., G. S. Nolas, G. A. Slack, A. C. Ehrlich, D. J. Gillespie, and G. L. Cohn, *J. Appl. Phys.* **79**, 8412 (1996).
Tu, Z. K., X. Sun, X. Li, R. X. Li, L. L. Xi, and J. Yang, *AIP Adv.* **9**, 045325 (2019).
Tütüncü, H. M., E. Karaca, and G. P. Srivastava, *Phys. Rev. B* **95**, 214514 (2017).
Uher, C., in *Thermoelectric Skutterudites*, CRC Press, Taylor & Francis, Boca Raton, FL (2021).
Vaqueiro, P., G. G. Sobany, A. V. Powell, and K. S. Knight, *J. Solid State Chem.* **179**, 2047 (2006).
Vaqueiro, P., G. G. Sobany, and M. Stindl, *J. Solid State Chem.* **181**, 768 (2008).

Volja, D., B. Kozinski, A. Li, D. Wee, N. Marzari, and M. Fornari, *Phys. Rev. B* **85**, 245211 (2012).
Wan, S., P. F. Qiu, X. G. Huang, Q. F. Song, S. Q. Bai, X. Shi, and L. D. Chen, *ACS Appl. Mater. Interfaces* **10**, 625 (2018).
Wang, H. T., B. Duan, G. H. Bai, J. L. Li, Y. Yu, H. J. Yang, G. Chen, and P. C. Zhai, *J. Electron. Mater.* **47**, 3061 (2018).
Wei, W., Z. Y. Wang, L. L. Wang, H. J. Liu, R. Xiong, J. Shi, H. Li, and X. F. Tang, *J. Phys. D: Appl. Phys.* **42**, 1 (2009).
Wojciechowski, K. T., *J. Alloys Compd.* **439**, 18 (2007).
Xing, G. Z., X. F. Fan, W. T. Zheng, Y. M. Ma, H. L. Shi, and D. J. Singh, *Sci. Rep.* **5**, 10782 (2015).
Yan, B., L. Müchler, X.-L. Qi, S.-C. Zhang, and C. Felser, *Phys. Rev. B* **85**, 165125 (2012).
Yang, X. X., Z. H. Dai, Y. C. Zhao, W. C. Niu, J. Y. Liu, and S. Meng, *Phys. Chem. Chem. Phys.* **21**, 851 (2019).
Zevalkink, A., K. Star, U. Aydemir, G. J. Snyder, J.-P. Fleurial, S. Bux, T. Vo, and P. von Allmen, *J. Appl. Phys.* **118**, 035107 (2015).
Zhang, L., B. Xu, X.-D. Li, F.-F. Duan, X.-L. Yan, and Y.-J. Tian, *Mater. Lett.* **139**, 249 (2015).

2 Superconducting Skutterudites

2.1 INTRODUCTION

Superconductivity is surely one of the most mysterious discoveries ever made. It must have been a great shock to Kamerlingh Onnes (1911) in his laboratory at the University of Leiden in Holland to see that his mercury sample apparently lost all its resistance when cooled down to near 4.5 K. It took several months and many experiments with other metallic samples before he was convinced that what he was observing is a genuine effect and not a glitch in the experimental setup. For a number of years, Kamerlingh Onnes was "the king of the world" with no competitors being able to liquefy helium and perform experiments below 10 K. For his low-temperature work and liquefaction of helium, he received the Nobel Prize in 1913. Perhaps not as dramatic but equally important was the discovery of the exclusion of magnetic flux from the interior of a metal some 20 years later by Meissner and Ochsenfeld (1933) as the metal underwent a transition to the superconducting state. The two effects, complete loss of resistance and flux exclusion, are macroscopic revelations of the mysterious phenomenon of superconductivity.

From our time in the middle school, we all know that electrons are negatively charged particles and, as such, repel each other by the Coulomb force. The essence of superconductivity is the formation of the so-called Cooper pairs whereby two electrons, under the right circumstances, bind together over a short distance called the coherence length ξ (a few tens to a few hundreds of nm, the latter value applicable to pure elemental superconductors), overcoming their Coulomb repulsion. In a simplistic but substantially correct picture of how such attractive interaction between two electrons arises, one can imagine an electron moving through a lattice of positively charged ions. The lattice gets polarized by the passage of the electron; i.e., the ions are drawn closer to the negative electron. However, because the ionic motion is retarded, meaning that the ions move much slower than electrons because of their nearly 2000 times heavier mass, the electron will be some 100–1000 nm ahead of the maximally perturbed ionic lattice. The locally greater density of positive ions thus attracts the second electron, effectively coupling the two electrons as they form a Cooper pair. The strength of this coupling is expressed by the electron–phonon coupling constant λ_{e-p}. In the Bardeen–Cooper–Schrieffer (BCS) theory, the Cooper pairs involve two electrons with opposite momenta $+\vec{k}$ and $-\vec{k}$ and opposite spins $\uparrow$ and $\downarrow$ (spin singlet). The requirement of opposite momenta implies that the orbital angular momentum $\vec{L}$ of the Cooper pair is zero, and because the paired electrons have opposite spins, so the spin angular momentum $\vec{S}$ is equal to zero. Consequently, the total angular momentum $\vec{J} = \vec{L} + \vec{S}$ is also zero. All Cooper pairs thus have the same zero total momentum, form a condensate of boson particles (particles with integer spin), and can be described by a macroscopic wavefunction Ψ. Superconductivity of this kind is referred to as the conventional *s*-wave superconductivity. The key finding of BCS theory is that Cooper pairs here have lower energy than two single electrons and are energetically separated by the superconducting gap 2Δ of the order of 10^{-4} – 10^{-3} eV. Consequently, superconductivity requires a low-temperature environment where the Cooper pairs are not destroyed by thermal energy (vibrations) of the crystal lattice. Apart from the coherence length, the properties of a superconductor are further characterized by the London penetration depth, λ, which indicates the distance in the interior of a superconductor over which the magnetic field drops to 1/e of the value it has at the surface. Typical values of the penetration length are in the range of 50 to 500 nm. The ratio of the penetration length and the coherence

DOI: 10.1201/9781003225898-2

length is called the Ginzburg–Landau (GL) parameter $\kappa = \lambda/\xi$, and it characterizes another peculiar aspect of superconductivity, namely, that certain superconductors remain superconducting even though pierced by an array of parallel narrow tubes (vortices) of the normal conducting state. The vortices first appear at the so-called lower critical magnetic field H_{c1} and grow in density as the magnetic field increases, and only at the upper critical magnetic field, H_{c2} is the superconductivity destroyed as the normal state takes over the entire volume of the sample. The magnitude of the GL parameter κ is used to classify superconductors into two categories. Superconductors for which $\kappa < 1/\sqrt{2}$ are called type-I superconductors and, except for niobium, vanadium, and technetium, are all elemental superconductors. In contrast, superconductors for which $\kappa > 1/\sqrt{2}$ are type-II superconductors and include all other superconducting structures, among them all superconducting skutterudites. The essential distinction between the two classes of superconductors is sketched in the phase diagrams in Figure 2.1.

The fundamental requirement for the *s*-wave superconductivity is a particular symmetry of the system. Specifically, the structure must possess inversion symmetry (imagine a mirror placed in the center of the structure) and time-reversal symmetry (TRS). The latter, a fancy sounding name, expresses the fact that the physical phenomena related to the structure should proceed in the same fashion when the arrow of time is reversed, $t \rightarrow -t$. If either of the two or both above symmetries are broken, the system belongs to the realm of unconventional superconductivity, characterized by the formation of nodes and lines of nodes on the Fermi surface where the superconducting gap function Δ_k becomes zero. Electrons at and close to such locations in k-space possess highly unusual properties, such as large effective masses (heavy fermions). Superconductors with broken TRS are often referred to as chiral superconductors. The excitement regarding the properties of chiral superconductors arises from a possibility that their electrons, given the right circumstances, can become their own antiparticles, referred to as Majorana fermions, the concept borrowed from high energy particle physics, Majorana (1937). While most superconductors and for that matter, most superconducting skutterudites are conventional *s*-wave superconductors, we shall see that there are some, particularly $PrOs_4Sb_{12}$, that show exotic behavior, including perhaps the best

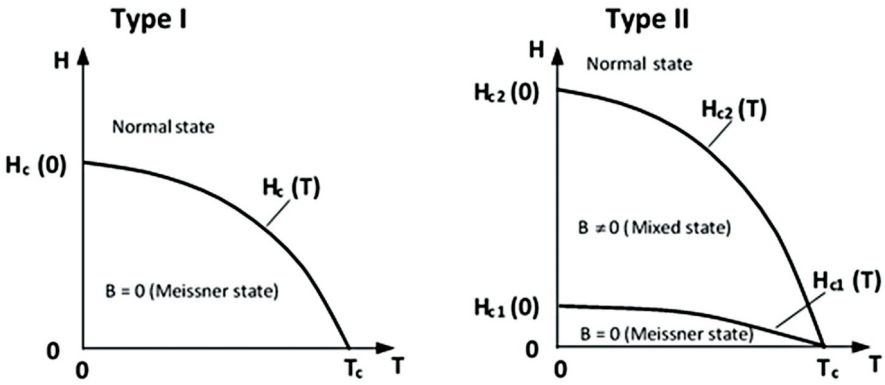

FIGURE 2.1 Schematic illustration of type-I and type-II superconductors. The superconducting state of a type-I superconductor is characterized by complete exclusion of flux (Meissner state). Its superconductivity is destroyed by magnetic field at the critical field $H_c(T)$. The highest magnetic field the type-I superconductor can survive is $H_c(0)$, the value at $T = 0$ K. In type-II superconductors, the Meissner state is destroyed; i.e., the vortices start to penetrate the superconductor, at a lower critical field $H_{c1}(T)$. However, superconductivity survives and is destroyed only at a higher critical field $H_{c2}(T)$. The highest magnetic field the type-II superconductor can withstand is $H_{c2}(0)$, the value at $T = 0$ K. The field range between H_{c1} and H_{c2} is called the mixed state of a superconductor.

prospect for harboring the Majorana fermions, Kozii et al. (2016). This has generated tremendous interest and fascination, provided theorists with innumerable opportunities to construct theoretical models to describe the novel physical phenomena, and offered experimentalists the challenging tasks of verifying them.

2.2 USEFUL RELATIONS FOR SUPERCONDUCTING PARAMETERS

In the analysis of experimental data, one aims to extract the key parameters characterizing the superconducting state. To achieve this aim, I summarize here several important relations I will refer to in the subsequent sections. Before I do so, a comment is in order regarding the use and dimension of a magnetic field, an important physical parameter when describing a superconducting state. A magnetic field $\boldsymbol{H}$ is a vector measured in units of Amperes per meter and represents the applied field, such as generated by a coil. Its value is unchanged whether or not a magnetic substance is placed inside the coil. In contrast, a magnetic induction $\boldsymbol{B}$, also called a magnetic flux density, is a vector measured in units of Tesla and depends on the spatial distribution of all circulating electrical currents, both those in the coil and those in any magnetic medium placed inside the coil. In free space (empty coil), $\boldsymbol{B}$ and $\boldsymbol{H}$ are identical, except for their respective units, and $\boldsymbol{B} = \mu_0\boldsymbol{H}$, where μ_0 is the permeability of free space, $4\pi \times 10^{-7}$ kgms^{-2}A^{-2} (Henry per meter). Magnetization $\boldsymbol{M}$, defined as the magnetic moment $\boldsymbol{m}$ per volume of sample V, has the same dimension as $\boldsymbol{H}$, i.e., Am^{-1}. In the presence of a magnetic material with magnetization $\boldsymbol{M}$ inside the coil, the magnetic induction becomes $\boldsymbol{B} = \mu_0(\boldsymbol{H} + \boldsymbol{M})$. It is a common practice to write and quote the lower and the upper superconducting critical fields, H_{c1} respectively H_{c2}, in units of Tesla (which, in fact, is $\mu_0 H$) rather than in strictly correct Amperes per meter. Magnetic susceptibility $\chi = M/H$ (a dimensionless quantity) relates the sensitivity of a material to magnetization M in the presence of the applied magnetic field H. The Meissner state (complete flux exclusion) has the susceptibility $\chi = -1$ in SI units and $\chi = -1/4\pi$ in cgs units. One often encounters a term "emu", which is an abbreviation for electromagnetic unit. Although it is not a unit in the conventional sense, the frequently quoted volume magnetization in cgs units, emu per cm^3, is equivalent to 10^3 Am^{-1} in SI units. More details of various susceptibilities and their conversion factors can be found in Chapter 3, describing magnetism in skutterudites.

The electron–phonon coupling constant λ_{e-p} that underpins the BCS theory is given by the product of the density of electronic states at the Fermi level $N(E_F)$ and the net-attractive potential between electrons at the Fermi surface V_0. This potential has an attractive electron–phonon part measured by λ_{e-p} and a repulsive screened Coulomb part μ_c*. Superconductors are classified as weak-coupling ($\lambda_{e-p} << 1$), intermediate-coupling ($\lambda_{e-p} \sim 1$), and strong-coupling ($\lambda_{e-p} >> 1$) superconductors. The coupling constant λ_{e-p} responsible for the attractive part of the Cooper pair bonding can be obtained from the McMillan (1968) formula relating it to the transition temperature T_c as

$$T_c = \frac{\theta_D}{1.45} exp\left[\frac{-1.04\left(1+\lambda_{e-p}\right)}{\lambda_{e-p} - \mu_c^*\left(1+0.62\lambda_{e-p}\right)}\right], \tag{2.1}$$

where θ_D is the Debye temperature, and the repulsive screened Coulomb part μ_c* is usually taken as equal to 0.13.

One of the important and readily measured parameters is the upper critical field $H_{c2}(T)$ at which the superconducting state is destroyed and the sample reverts to the normal state. The maximum value of $H_{c2}(T)$ is attained at absolute zero temperature and is designated as $H_{c2}(0)$. Because achieving a temperature near 0 K is quite challenging, there is a useful relation, referred to as the WHH

formula, standing for Werthamer–Helfand–Hohenberg (1966), that relates $H_{c2}(0)$ in units of Tesla to the initial slope of the T-dependent upper critical field in units of TK^{-1} taken at the transition temperature T_c,

$$H_{c2}^{orb}(0) = 0.693 T_c \left(-\frac{dH_{c2}(T)}{dT} \right)_{|T_c} . \tag{2.2}$$

The upper critical field in Equation 2.2 expresses the resistance of the Cooper pairs against their destruction by the orbital motion of electrons. While the superscript "*orb*" is included in Equation 2.2 to indicate that the upper critical field here refers to the orbital pairbreaking mechanism, it will be dropped in subsequent discussions. One also often encounters the upper critical field that describes the ability of the Cooper pairs to withstand a spin flip of one of its electrons, referred to as the Pauli paramagnetic-limited upper critical field or, equivalently, as the Clogston–Chandrasekhar limit. The latter critical field $H_{c2}^{p}(0)$ is higher and in units of Tesla is given by

$$H_{c2}^{P}(0) = 1.84 \left(TK^{-1} \right) T_c . \tag{2.3}$$

The experimentally extrapolated upper critical fields of superconducting skutterudites lie much closer to the orbital estimate of Equation 2.2 than to the Pauli limited value given by Equation 2.3.

Once $H_{c2}(0)$ is known, the coherence length ξ_0 (in meters) can be obtained from, e.g., Tinkham (1983), as

$$\xi_0 = \left(\frac{\Phi_0}{2\pi H_{c2}(0)} \right)^{1/2}, \tag{2.4}$$

where $\Phi_0 = h/2e \approx 2.07 \times 10^{-15}$ Tm^2 is the flux quantum.

The Fermi velocity of electrons v_F is related to the coherence length ξ_0 through

$$v_F = \frac{\xi_0 k_B T_c}{0.18\hbar}. \tag{2.5}$$

Assuming a simple spherical Fermi surface, the Fermi wave-vector k_F is given by

$$k_F = \left(\frac{3\pi^2 Z}{\Omega} \right)^{1/3}, \tag{2.6}$$

where Z is the number of electrons in the unit cell (in the case of superconducting skutterudites filled with Pr this means that two cages per unit cell each with three electrons from the Pr^{3+} ion for a total of Z = six electrons) and Ω is the volume of the unit cell taken as the lattice constant to the power of three. Using Equations 2.5 and 2.6, the effective mass m^* follows from

$$m^* = \frac{\hbar k_F}{v_F}. \tag{2.7}$$

The electronic specific heat coefficient (Sommerfeld coefficient) γ_n is then obtained from

$$\gamma_n = \pi^2 \left(\frac{Z}{\Omega} \right) \frac{k_B^2}{\hbar k_F^2} \; m^*. \tag{2.8}$$

At zero temperature, the penetration depth is given by Gross et al. (1986) in the form

$$\lambda(0) = \frac{\left[\Phi_0 H_{c2}(0) \right]^{1/2}}{\sqrt{24}\, \delta_{sc} T_c \gamma_n^{1/2}}, \tag{2.9}$$

where $\delta_{sc} \equiv \Delta(0)/k_B T_c$, with $\Delta(0)$ being the superconducting band gap at zero temperature. In the BCS theory, the band gap at $T = 0$ K is given by

$$\Delta(0) = 1.76\, k_B T_c, \tag{2.10}$$

and its temperature dependence close to T_c is of the form

$$\Delta(T) = 3.06\, k_B T_c \left(1 - \frac{T}{T_c} \right)^{1/2}. \tag{2.11}$$

In zero magnetic field, the superconducting transition is a second-order phase transition, and, as such, the entropy $S(T)$ at T_c does not change. However, its derivative, related to the specific heat $C(T) = TdS(T)/dT$, experiences a jump at the critical temperature designated as $\Delta C \equiv C_s - \gamma_n T$, where the term $\gamma_n T$ is the electronic specific heat in the normal state. The coefficient of the electronic specific heat γ_n is also directly related to the density of electronic states at the Fermi level,

$$\gamma_n = \frac{\pi^2}{3} D(E_F) k_B^2. \tag{2.12}$$

At the critical temperature T_c, the BCS theory predicts a jump in the specific heat of

$$\Delta C(T_c) = 4.68\, D(E_F) k_B^2 T_c. \tag{2.13}$$

From Equations 2.12 and 2.13, the normalized jump in the specific heat at T_c is then a parameter-free expression in the BCS theory of magnitude

$$\frac{\Delta C(T_c)}{\gamma_n T_c} = 1.43. \tag{2.14}$$

In the BCS theory, the uniform energy gap $E_g = 2\Delta$ implies that the specific heat decreases exponentially with the decreasing temperature and is proportional to

$$C_s(T) \propto e^{-1.76 \frac{T_c}{T}}. \tag{2.15}$$